Loughborough University

This item was submitted to Loughborough's Research Repository by the author.
Items in Figshare are protected by copyright, with all rights reserved, unless otherwise indicated.

Explicit and implicit large eddy simulations of free jets

PLEASE CITE THE PUBLISHED VERSION

LICENCE

CC BY-NC 4.0

REPOSITORY RECORD

Kuan, Tzuo Wei It, Francesco Cocetta, and Joanna Szmelter. 2021. “Explicit and Implicit Large Eddy Simulations of Free Jets”. Loughborough University. https://doi.org/10.17028/rd.lboro.14588553.v1.

Explicit and Implicit Large Eddy Simulations of Free Jets

Tzuo Wei It Kuan[1*], Francesco Cocetta[1], Joanna Szmelter[1]

[1] Wolfson School of Mechanical, Electrical and Manufacturing Engineering,
Loughborough University, Loughborough, LE11 3TU, UK.
t.w.i.kuan@lboro.ac.uk, f.cocetta@lboro.ac.uk, j.szmelter@lboro.ac.uk

Abstract

The paper presents studies of a turbulent free jet focusing on the comparison of the efficiency and accuracy obtained using the Large Eddy Simulation (LES) and the Implicit Large Eddy Simulation (ILES) approaches. The solutions are obtained by solving the incompressible Navier-Stokes equations using an unstructured mesh-based Non-oscillatory-Forward-in-Time (NFT) integration framework [1, 2]. The integration builds upon the second-order-accurate high-resolution Multidimensional Positive Definite Advection Transport Algorithm (MPDATA). The capabilities to adequately capture essential turbulent free jet features in both the LES and ILES approaches are demonstrated in the presented work, with the LES simulations carried out at Reynolds number $Re = 1.0 \times 10^4$. Both approaches show good agreement when compared against experiments of Panchapakesan et al. [3] and Hussein et al. [4], with the ILES approach showing a better prediction of the near-field development of the jet. The flexibility of the numerical scheme is also highlighted through numerical investigations with different mesh topologies.

Key words: *Turbulent Free Jets, Implicit Large Eddy Simulation, MPDATA*

1 Introduction

The advancement in computational power within the recent decade meant that LES has become more affordable for simulating a broad range of engineering applications. The capabilities of capturing the dynamics of large-scale unsteady motions can certainly improve predictions of jet flow behaviour such as spreading rate and turbulent mixing characteristics. Understanding these phenomena is crucial for the systematic design of engineering applications of jets. The present work adopts the NFT MPDATA numerical scheme to simulate turbulent free jets. Among the properties of MPDATA are the sign-preservation of scalar quantities, the nonlinear stability of the simulation, and the suppression of unphysical oscillations. Moreover, MPDATA exhibits ILES capabilities whereby the viscous effects would implicitly arise from the truncation terms within the numerical scheme. The presented results intend to first provide a general validation for the NFT MPDATA scheme through the conventional LES approach, followed by an illustration of ILES capabilities based on the NFT MPDATA scheme and comparison with experiments. Then, results based on identical numerical setup but with different mesh topologies are compared.

2 Numerical approach and problem description

The present work adopts the unstructured mesh-based NFT framework to integrate the governing equations for isothermal, homogeneous, incompressible Navier-Stokes equations. Key components of the adopted NFT framework are the MPDATA scheme which acts as the advection operator, and a robust non-symmetric Krylov-subspace solver that solves the resulting elliptic Poisson problem implied by the mass-continuity constraint. The spatial discretisation uses median-dual finite volumes and an edge-based data structure providing flexibility to integrate the governing equations over arbitrarily shaped cells. In the LES approach, the Smagorinsky-like subgrid-scale (SGS) model within Spalart-Allmaras DES turbulence model is employed to explicitly provide the required eddy viscosity for closure. Descriptions of both solution procedure and the explicit SGS treatment are provided in [1]. In the ILES approach, the SGS effects are implicitly applied through MPDATA, in fact, in the limit of high Reynolds number flows presented in the current work, the viscous terms are omitted when integrating the governing equations. In this case, the self-regularisation property of MPDATA will reverse the filtering process within the low-order upwinding of the MPDATA iterative process, effectively resulting in the leading-order truncation terms to be dissipative and operate as a higher-order filter [1].

The free jet simulations are computed in a cuboidal domain of dimensions $[-6,6]\times[-6,6]\times[0,30]$ m^3 with a round jet of reference inlet diameter $d \approx 1.00\,m$ discharged at the centre of the inlet plane at the top of the domain, i.e. (0,0,30) m. Three different meshes have been tested: a uniformly distributed Cartesian mesh (MT-CART-UF), a uniform triangular-based prismatic mesh (MT-PRIZ-UF), and a triangular-based prismatic mesh with coarsening towards the lateral boundaries (MT-PRIZ-CS). All meshes have a base discretisation of $dz = 0.125\ m$ in the vertical direction and $dx = dy = 0.100\ m$ in the horizontal directions. On the inlet plane, jet velocity of $W_0 = -1.00$ ms^{-1} is applied within the jet inlet region, mimicking the top-hat profile described in [3], and a co-flow of $w_{cf} = -0.04\ ms^{-1}$ is prescribed in the remaining part of the inlet boundary plane. The purpose of the co-flow is to provide entrainment fluid for the jet and to suppress any large scale circulation at the outlet. Additionally, to aid the jet in transitioning into its intermediate field, normally distributed random noise with a root mean square of 3% in the axial direction of the jet and 1% in the tangential directions is continuously added onto two nodal layers from the jet inlet. The outflow boundary condition strategy includes a combination of a moderately weak absorber applied at 6 m above the outlet plane to attenuate vortical structures to the Convective Boundary Condition (CBC) [5] prescribed at the outlet. A Gaussian velocity profile is used as the target for the absorber and the same profile is also prescribed as the convective velocity for the CBC condition. It is noted that the amplitude of the selected Gaussian velocity profile is needed to be tuned on a case by case basis and the overall profile is selected to conserve the global mass-continuity. Free-slip boundary conditions are applied on the remaining lateral faces. The time-step is set to $dt = 1.25\times10^{-2}s$.

3 Numerical results

Firstly, we compare the results of LES and ILES approaches obtained on the same Cartesian mesh. Figure 1 shows the centerline decay characteristics of the two cases plotted alongside the experimental data fit provided in [3]. To account for the effects of co-flow, the simulated centerline decay characteristics are plotted as a function of the excess centerline mean velocity, i.e. $(< W_c(z) > -w_{cf})$ yielding a centerline decay expression, $(W_0 - w_{cf})/(< W_c(z) > -w_{cf}) = (1/B)(z/d - z_0/d)$ where B is the centerline decay constant, z_0/d is the normalised virtual origin, and $< W_c(z) >$ is the time-averaged centerline velocity at a given axial position away from the inlet plane, z. Furthermore, one-dimensional energy spectra, E_{11}, calculated from the autocorrelation function based on the time-series axial velocity fluctuation at various axial position on the centerline are presented in Figures 2 and 3 for LES and ILES, respectively. The analysis is similar to those by Fellouah et al. [6] but the presented spectra are not normalised against Kolmogorov scales due to the non-trivial nature of quantifying viscosity in the ILES case. Instead, dimensional E_{11} are plotted against the wavenumber, $\kappa_1 = 2\pi f/ < W >$ where f is the frequency. Hanning window has also been applied to reduce spectral lobe leakage in the Fast Fourier Transformation.

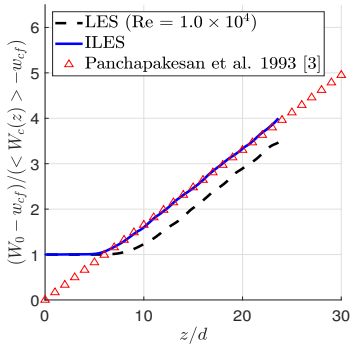

Figure 1: Centerline decay

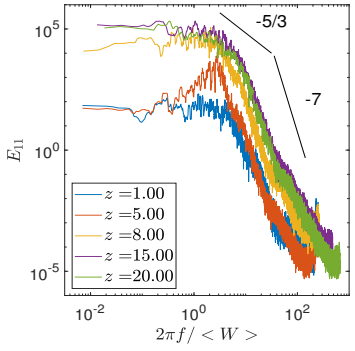

Figure 2: 1D Energy Spectra for LES

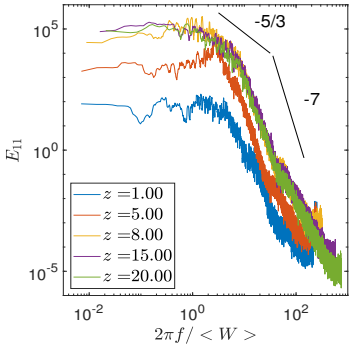

Figure 3: 1D Energy Spectra for ILES.

The key comparison focuses on the linear relationship within the intermediate field of the jet seen

in Figure 1, where the jet has begun to develop towards its self-similar state in the far-field. From Figure 1, $B = 6.05$ and $B = 5.94$ as well as $z_0/d = 2.610$ and $z_0/d = 0.262$ were obtained for LES and ILES respectively. Both characteristics decay rates B compare very well with the linear fit in [3] where $B = 6.06$ was determined. On the other hand, overprediction of the potential core length is observed in the LES results when compared to experimental data in [3], however, a better prediction is obtained with the ILES approach. Insights on the potential core decay can also be drawn from the energy spectra in Figure 2 and Figure 3 whereby dominant wavenumbers are observed to be more energetic and occur at earlier axial positions for ILES than LES. These show that the LES approach does not evolve the jet within its near-field region as quickly as the ILES approach. Further to that, in both cases, energy spectra within the intermediate field exhibit the -5/3 gradient that signifies the inertia subrange as well as exhibit the -7 gradient that characterises viscous dissipation [6]. These trends are also observed in [6] and thus adding validation merits to the two approaches. More importantly, the analysis highlights the fact that the ILES approach is capable of capturing the inertia subrange and dissipation range despite the omission of the viscous terms in its formulation.
Additionally, self-similar profiles obtained through conical averaging within the intermediate field are compared against experimental data [3, 4] in Figures 4a to 4c. The presented results adopt the same self-similar coordinates formalisation as in [4] and the velocity components are normalised with respect to the excess centerline mean velocity, i.e. $(< W_c(x) > -w_{cf})$.

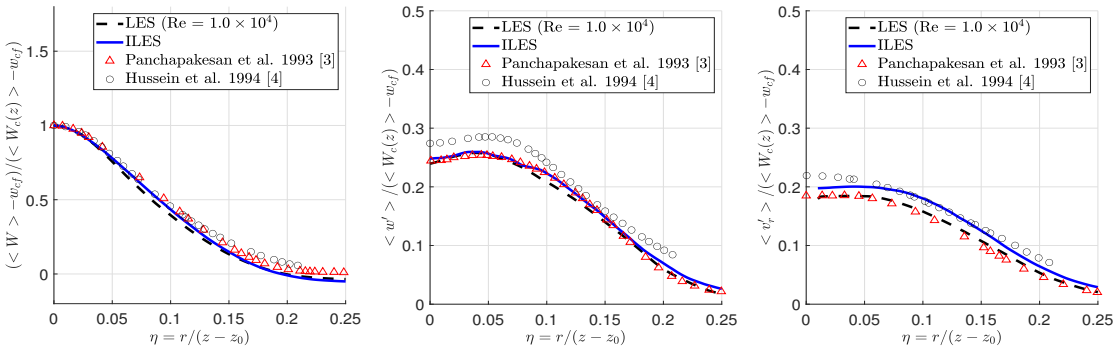

(a) Mean axial velocity (b) Axial velocity fluctuation (c) Radial velocity fluctuation

Figure 4: Comparison of self-similar profiles between LES ($Re = 1.0 \times 10^4$) and ILES.

The LES results show strong agreement with the self-similar profile obtained by Panchapakesan et al. [3]. Minor discrepancies between the LES data and experimental data may be due to the evaluation of the self-similar state within the intermediate field instead of the far-field region of the jet. It should be pointed out that attaining the true self-similar profile from axial positions processed in [3] or [4] would certainly be computationally costly. Impressively, the ILES approach also reproduces similar results when compared to LES and experimental data [3, 4]. The impact of ILES representing higher Reynolds number flow is also seen through the observation whereby the self-similar profiles tends towards experimental data of Hussein et al. [4]. It is noted that the experimental data of Hussein et al. [4] represents an experiment with Reynolds number one order higher than Reynolds number used in the Panchapakesan et al. [3] experiment. These observations alongside the centerline characteristics and trends in the energy spectra further strengthen the validity of the NFT MPDATA scheme in both the LES and ILES approaches. Furthermore, the ILES approach achieved a 17% computational cost saving in contrast to the LES approach.
Lastly, the flexibility of the numerical scheme is demonstrated by repeating the LES simulation under similar boundary conditions but with the previously described prismatic triangular meshes. The centerline decay characteristics, as well as the self-similar axial and radial velocity fluctuation profiles, are plotted and shown in Figures 5a to 5c.
The characteristics decay rates B were found to be similar among the three meshes but the prismatic triangular meshes are able to trigger an earlier development of the jet into the intermediate

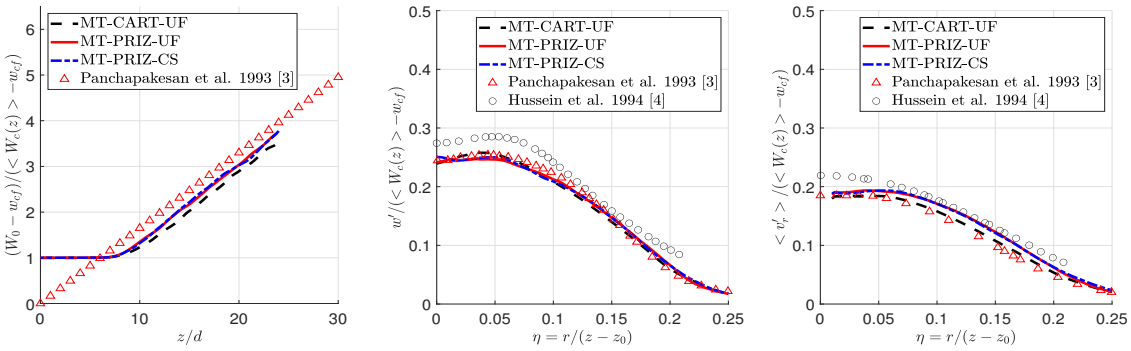

(a) Centerline decay (b) Axial velocity fluctuation (c) Radial velocity fluctuation

Figure 5: Comparison of free jets characteristics for different mesh topologies.

field in contrast to the uniform Cartesian mesh. The axial velocity fluctuation has shown to coincide with one another which is not unexpected since all three meshes are axially extended in a similar manner, however, there are some observable differences in the radial velocity fluctuation. The differences, in the centerline decay characteristics and radial velocity fluctuation, are most likely due to the induction of flow solution perturbation akin to random noise as a result of prismatic triangular cells rather than a reduction in molecular diffusion.

4 Conclusions

The LES and ILES approaches based on the NFT MPDATA scheme employed to simulate the turbulent free jet have been validated, with both approaches showing good agreement when compared with experimental data [3, 4]. The ILES approach appears to be particularly useful, as it enables the representation of high Reynolds number flows without the need for explicit SGS models.

Acknowledgments

This work was supported in part by the funding received from the EPSRC studentship grant 1965773, and Horizon 2020 Research and Innovation Programme (ESCAPE2 grant agreement no. 800897). The Lovelace HPC services were provided at Loughborough University.

References

[1] J. Szmelter, P.K. Smolarkiewicz, Z. Zhang, Z. Cao (2019): Non-oscillatory forward-in-time integrators for viscous incompressible flows past a sphere, *J. Comput. Phys.* 386, 365-383.

[2] P.K. Smolarkiewicz, J. Szmelter (2005): MPDATA: An Edge-Based Unstructured-Grid Formulation, *J. Comput. Phys.* 206, 624-649.

[3] N.R. Panchapakesan, J.L. Lumley (1993): Turbulence measurements in axisymmetric jets of air and helium. Part 1. Air jet. *J. Fluid Mech.* 246, 197-223.

[4] H.J. Hussein, S.P. Capp, W.K. George (1994): Velocity measurements in a high-Reynolds-number, momentum-conserving, axisymmetric, turbulent jet. *J. Fluid Mech.* 258, 31-75.

[5] I Orlanski (1976): A simple boundary condition for unbounded hyperbolic flows. *J. Comput. Phys.*, vol. 21(3), 251-269.

[6] H.Fellouah, A.Pollard (2009): The velocity spectra and turbulence length scale distributions in the near to intermediate regions of a round free turbulent jet *Phys. Fluids*, vol. 21(11), 115101.